

SHORT REPORT

The GET pathway can increase the risk of mitochondrial outer membrane proteins to be mistargeted to the ER

Daniela G. Vitali¹, Monika Sinzel¹, Elianne P. Bulthuis^{1,*}, Antonia Kolb¹, Susanne Zabel¹, Dietmar G. Mehlhorn², Bruna Figueiredo Costa^{3,‡}, Ákos Farkas⁴, Anne Clancy⁴, Maya Schuldiner⁵, Christopher Grefen², Blanche Schwappach⁴, Nica Borgese³ and Doron Rapaport^{1,§}

ABSTRACT

Tail-anchored (TA) proteins are anchored to their corresponding membrane via a single transmembrane segment (TMS) at their C-terminus. In yeast, the targeting of TA proteins to the endoplasmic reticulum (ER) can be mediated by the guided entry of TA proteins (GET) pathway, whereas it is not yet clear how mitochondrial TA proteins are targeted to their destination. It has been widely observed that some mitochondrial outer membrane (MOM) proteins are mistargeted to the ER when overexpressed or when their targeting signal is masked. However, the mechanism of this erroneous sorting is currently unknown. In this study, we demonstrate the involvement of the GET machinery in the mistargeting of suboptimal MOM proteins to the ER. These findings suggest that the GET machinery can, in principle, recognize and guide mitochondrial and non-canonical TA proteins. Hence, under normal conditions, an active mitochondrial targeting pathway must exist that dominates the kinetic competition against other pathways.

KEY WORDS: ER, GET, Mitochondria, Outer membrane, Protein sorting, Tail-anchor

INTRODUCTION

Eukaryotic cells face the challenge of directing newly synthesized membrane proteins to the right compartment because their mistargeting not only leads to their absence in the target organelle but also burdens the cytosol with aggregates of such proteins. Two main destinations for such proteins are mitochondria and the endoplasmic reticulum (ER). The mechanisms for targeting each membrane protein to its correct membrane depend on the protein topology and the targeting signals it contains.

Hundreds of eukaryotic membrane proteins have a single α -helical transmembrane segment (TMS) at their C-terminus (Kalbfleisch et al., 2007). The import of these proteins to the ER can be mediated by the guided entry of tail-anchored (TA) proteins (GET) pathway (Schuldiner et al., 2008). The recognition happens

immediately after the release of the protein from the ribosome by the pre-targeting complex, which comprises Sgt2, Get4 and Get5. Sgt2 binds the TMS and discriminates between mitochondrial and ER TA proteins (Wang et al., 2010). Sgt2 then hands over the substrate to the Get4–Get5 complex that, in turn, recruits Get3, a cytosolic chaperone. Get3 shuttles TA proteins to the ER membrane, where Get1 and Get2 form a receptor complex that recognizes the Get3-TA protein complex and facilitates the release of the TA proteins (Schuldiner et al., 2008). It appears that the Get1-Get2 receptor can mediate the membrane insertion of some TA proteins (Wang et al., 2011), however, other TA proteins with a moderately hydrophobic TMS, as e.g. cytochrome b5 and the protein tyrosine phosphatase PTP1B, can spontaneously insert into the lipid bilayer (Brambillasca et al., 2005; Colombo et al., 2009). Recently, an additional ER membrane protein targeting pathway was identified, which can compensate the absence of either the signal recognition particle (SRP) or of the GET machinery and was named SRP-independent targeting (SND) pathway (Aviram et al., 2016; Hassdenteufel et al., 2017).

TA proteins are also targeted to the mitochondrial outer membrane (MOM), but none of the known mitochondrial import machineries are required for their insertion (Kemper et al., 2008; Dukanovic and Rapaport, 2011). It has been proposed that the difference in the lipid distribution (mainly of ergosterol) between ER and mitochondria plays a role in assuring specificity in targeting to mitochondria (Krumpe et al., 2012). Compared to ER-localized TA proteins, mitochondrial TA proteins generally have a moderately hydrophobic TMS flanked by positively charged residues. Despite these differences, the overall similarity of targeting signals between ER and mitochondrial destined TA proteins causes their mistargeting to the wrong organelles on different occasions. However, the mechanism by which mistargeting occurs is, so far, unresolved.

In this work, we used *Saccharomyces cerevisiae* to identify MOM proteins that are mislocalized to the ER because either their targeting sequence is masked or the membrane import machinery is saturated. We further demonstrate that their mistargeting to the ER membrane depends on the GET machinery, suggesting that under normal circumstances a mitochondrial targeting pathway counterbalances GET substrate capture.

RESULTS AND DISCUSSION**GET-dependent mislocalization of cytochrome b5-RR**

The mammalian TA protein cytochrome b5 has two isoforms; one (b5-ER) is located in the ER and the other (b5-OM) in the MOM (D'Arrigo et al., 1993). The ER isoform has a predominantly negatively charged C-terminus while the mitochondrial isoform is mostly positively charged. Replacement of the C-terminal segment of b5-ER with two arginine residues – yielding substitution mutant

¹Interfaculty Institute of Biochemistry, University of Tübingen, 72076 Tübingen, Germany. ²Centre for Plant Molecular Biology, Developmental Genetics, University of Tübingen, Tübingen 72076, Germany. ³Consiglio Nazionale delle Ricerche Institute of Neuroscience, Milan 20100, Italy. ⁴Department of Molecular Biology, Universitätsmedizin Göttingen, Göttingen 37073, Germany. ⁵Department of Molecular Genetics, Weizmann Institute of Science, Rehovot 7610001, Israel. ^{*}Present address: Department of Biochemistry, Radboud University Medical Centre, 6500HB Nijmegen, The Netherlands. [‡]Present address: Telomeres and Cancer Laboratory, Champalimaud Centre for the Unknown, 1400-038 Lisbon, Portugal.

[§]Author for correspondence (doron.rapaport@uni-tuebingen.de)

 D.R., 0000-0003-3136-1207

b5-RR – leads to re-direction of the protein to mitochondria (Borgese et al., 2001) (Fig. 1A).

To understand better the distribution of the two isoforms between both organelles, we expressed rabbit b5-ER and its b5-RR variant in yeast cells, and analysed their localization by subcellular fractionation. As expected, we found the vast majority of the ER form in the ER (microsomal) fraction of yeast cells and only marginal amounts in their mitochondria (Fig. 1B). Surprisingly, ~50% of the mitochondrial isoform was found in the ER fraction of yeast cells (Fig. 1C). This is in sharp contrast to the situation in mammalian cells where the vast majority of b5-RR is found in mitochondria (Borgese et al., 2001). Thus, it seems that those features that assure correct targeting in mammalian cells do not function properly in yeast cells. Similar differences between targeting in mammalian cells compared with that in yeast were observed for PTP1B and Bcl2. In mammalian cells, both proteins localize to the ER and mitochondria but are found, once expressed in yeast cells, solely in the ER (Egan et al., 1999; Fueller et al., 2015).

Furthermore, a substantial proportion of these b5-RR mistargeted molecules migrated at a higher than expected molecular mass, suggesting that they had been modified (Fig. 1C). To characterize the topology of the native and modified forms, we treated isolated microsomes with proteinase K. This treatment resulted in disappearance of the native protein signal suggesting that it adopted a classical TA topology. In contrast, the modified form

was protease resistant, unless the membrane was solubilized with detergent (Fig. 1D). This outcome raised the possibility that the modified form flipped its topology such that the N-terminus faces the microsome lumen. Moreover, by using alkaline extraction both native and modified microsomal forms of b5-RR, as well as b5-RR localized in mitochondria, were found to be integrated into membranes (Fig. 1E).

The inside-out topology of the modified b5-RR suggests that its modification might be glycosylation. Hence, we treated b5-RR-containing microsomes with either endoglycosidase H (EndoH) or peptide:N-glycosidase (PNGase). Both enzymes caused the disappearance of the modified form of b5-RR and of protein disulfide-isomerase (Pdi1), which served as a control. Of note, the NetNGlyc 1.0 Server (<http://www.cbs.dtu.dk/services/NetNGlyc/>), which predicts N-glycosylation sites, suggested Asp residue 21 of cytochrome b5 as a potential glycosylation site (Fig. 1A). We concluded that a considerable portion of b5-RR molecules was mistargeted to the ER and some of those molecules had been inserted in the opposite orientation, i.e. with the N-terminus in the lumen. These findings can be explained by recent reports suggesting that the SRP and the Sec translocon are involved in the targeting of some TA proteins, including cytochrome b5, to the ER (Casson et al., 2017; Hassdenteufel et al., 2017). Thus, it might be that the Sec translocon mediates an integration of a sub-population of b5-RR into the ER membrane in the wrong topology.

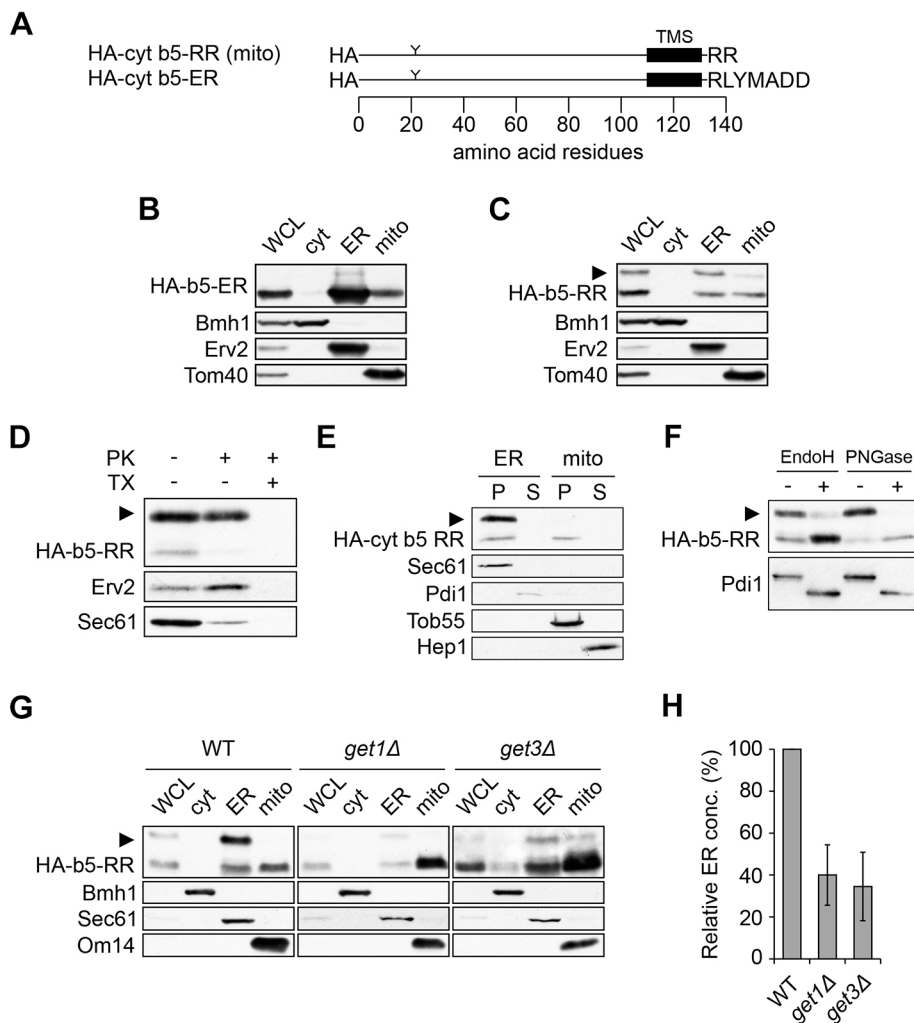


Fig. 1. Cytochrome b5-RR is partially mistargeted to ER in a GET-dependent manner. (A) Schematic representation of cytochrome b5 isoforms. Y represents a potential glycosylation site. (B,C) Whole-cell lysate (WCL) and fractions corresponding to cytosol (cyt), microsomes (ER) and mitochondria (mito) from cells expressing either b5-ER (B) or b5-RR (C) were analysed by SDS-PAGE and immunoblotting. (D) Western blot showing ER fractions treated with proteinase K (PK) in the absence or presence of Triton X-100 (TX). (E) Western blot showing ER and mitochondria fractions subjected to alkaline extraction. Pellet (P) and supernatant (S) fractions were analysed by SDS-PAGE and immunoblotting. (F) Western blot showing the ER fraction incubated in the presence (+) or absence (-) of either EndoH or PNGase. (G) Western blot showing WT, *get1Δ* and *get3Δ* cells expressing b5-RR subjected to subcellular fractionation and analysis as in (C). (H) Quantification of three independent experiments as in G; enrichment of the lower form of b5-RR in ER fractions is depicted. Arrowheads in C-G indicate the modified form of HA-b5-RR.

Since ER TA proteins can be targeted to their destination by the GET machinery (Borgese and Fasana, 2011; Schuldiner et al., 2008), we wondered whether this system can participate in the missorting of b5-RR. To test this, we expressed b5-RR in cells that lack the ER receptor Get1 or the cytosolic chaperone Get3. We observed that, in both deletion strains, a smaller proportion of b5-RR molecules localized to the ER, whereas higher amounts were found in mitochondria (Fig. 1G,H). These findings suggest that the GET machinery deviates this substrate from its natural target membrane. Of note, we observed that ~30-40% of b5-RR molecules are localized to ER, even in the absence of functional GET system. This partial dependence on the GET components is in line with the idea that multiple selection filters are used by the GET machinery to assure correct targeting (Rao et al., 2016), and that alternative pathways, involving SRP, hSnd2 and/or unassisted

membrane integration, exist for ER TA protein targeting in the absence of GET (Casson et al., 2017; Hassdenteufel et al., 2017).

The GET machinery mediates mistargeting of Mcp3

In *S. cerevisiae* the MOM protein Mcp3 follows a unique import pathway that involves the TOM and TIM23 complexes, as well as processing by the inner membrane peptidases 1 and 2 (Imp1/2) (Sinzel et al., 2016). Mcp3 contains a presequence-like segment in its N-terminal region, whereas the C-terminal half contains two putative TMSs, one of them very close to the C-terminus (Fig. 2A). When Mcp3 was N-terminally labelled with GFP, we observed considerable mislocalization to the ER (Fig. 2B), potentially due to masking of the presequence by the GFP moiety.

Of note, alkaline extraction confirmed that the GFP-tagged version was integrated into the membranes of either mitochondria or

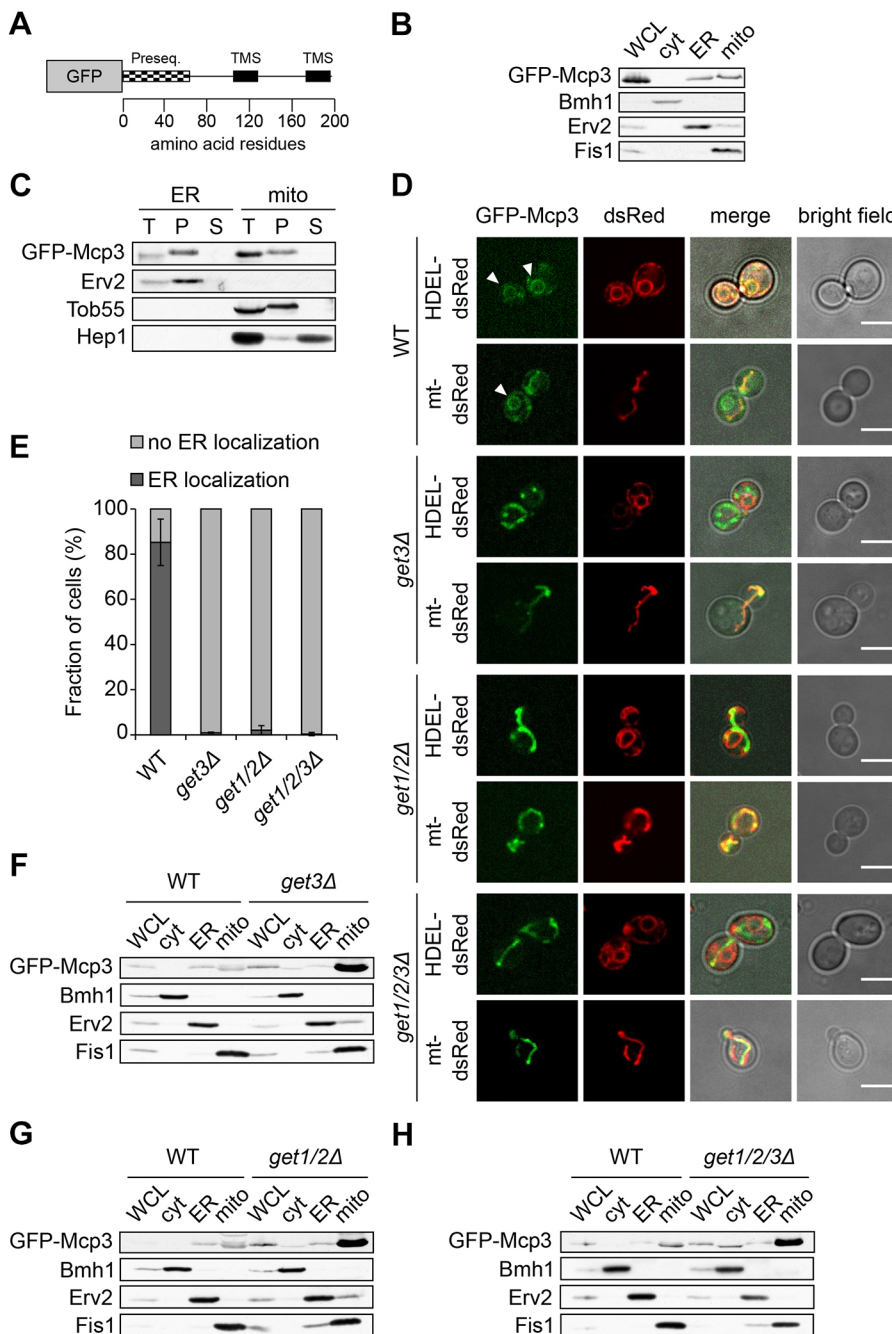


Fig. 2. The mistargeting of GFP-Mcp3 to ER requires the GET machinery. (A) Schematic representation of GFP-Mcp3. (B) Western blot showing cells expressing GFP-Mcp3 subjected to subcellular fractionation and analysis as described for Fig. 1B. (C) Western blot showing ER and mitochondrial fractions subjected to alkaline extraction as described for Fig. 1E. T, total; P, pellet; S, supernatant. (D) WT, *get3Δ*, *get1Δget2Δ*, and *get1Δget2Δget3Δ* cells expressing GFP-Mcp3 and either the ER marker HDEL-dsRed or the mitochondrial marker mt-dsRed were analysed by fluorescence microscopy and representative images are shown. Arrowheads indicate perinuclear ER localization. Scale bars: 5 μm. (E) Quantification of the intracellular localization of GFP-Mcp3 monitored as in D. The figure shows the average±s.d. of three independent experiments with at least 100 cells each. (F-H) Western blots showing WT, *get3Δ* (F), *get1/2Δ* (G), and *get1/2/3Δ* (H) cells expressing GFP-Mcp3 subjected to subcellular fractionation as described for Fig. 1B. WCL, whole-cell lysate; cyt, cytosol fraction; ER, microsomal fraction; mito, mitochondria fraction; WT, wild type.

the ER (Fig. 2C). Since Mcp3 has a TMS at its C-terminal region, we wondered whether GET components are required for its missorting. To address this point, we introduced GFP-Mcp3 into strains deleted for *GET3* alone (*get3Δ*), double-deleted for *GET1* and *GET2* (*get1/2Δ*), or triple deleted for *GET1*, *GET2* and *GET3* (*get1/2/3Δ*). Fluorescence microscopy verified the predominant ER localization of GFP-Mcp3 in WT cells. In sharp contrast, only negligible staining of the ER and a typical tubular pattern of mitochondria was observed in cells lacking one, two or all of the GET components (Fig. 2D,E).

To test our assumption that the N-terminal GFP interferes with the function of the presequence of Mcp3, we constructed a Mcp3 variant lacking its N-terminally presequence (Mcp3ΔN). Indeed, this construct behaved similarly to the GFP full-length Mcp3 and was localized to ER structures. This location disappeared upon deletion of either *GET1* or *GET3* (Fig. S1). However, in contrast to the full-length protein, the truncated variant, which lacks the mitochondrial targeting signal, was spread in the absence of the GET machinery in the cytosol or appeared in punctate structures, representing probably aggregated molecules (Fig. S1).

To support the fluorescence microscopy data, we performed subcellular fractionation of WT cells and *get* mutant cells expressing GFP-Mcp3. In all *get* mutant strains, we observed much higher amounts of GFP-Mcp3 in the mitochondrial fraction as compared to WT cells (Fig. 2F-H). Notably, the *get* mutant strains appear to contain a minor population of GFP-Mcp3 in their ER fraction. This, again, might be due to alternative targeting pathways supporting this rerouting but could also be due to cross-contamination between the ER and mitochondrial fractions. Markedly, the overall higher amounts of GFP-Mcp3 in the *get* mutants raise the possibility that GFP-Mcp3 is unstable in WT cells and undergoes degradation.

In summary, masking the mitochondrial targeting information in the N-terminal region with a GFP moiety probably slowed the association with mitochondria, thus providing the GET machinery a chance to recognize the C-terminal TMS of Mcp3 as a potential substrate. In the case of native Mcp3, the mitochondrial import is most likely so fast that it does not provide the GET machinery a time window to interfere with this process.

Overexpressed GFP-tagged Mim1 is partially targeted to the ER

The yeast mitochondrial import protein 1 (Mim1) is a MOM protein that harbours a central membrane-spanning hydrophobic stretch (Ishikawa et al., 2004; Waizenegger et al., 2005) (Fig. 3A). Subcellular fractionation indicated that, upon overexpression, GFP-Mim1 is mistargeted to the ER (Fig. 3B). It has been suggested that the GET pathway can also recognize TMSs that are not strictly at the C-terminus (Aviram et al., 2016), so it remained possible that it can even recognize proteins with a central TMS, like Mim1.

To understand better the mechanism of mistargeting, we first assayed whether the missorted overexpressed GFP-Mim1 is membrane-embedded, and observed that GFP-Mim1 behaved as a membrane protein in both ER and mitochondria fractions (Fig. 3C,D). We next investigated whether the ER localization is dependent on GET proteins. Hence, we expressed GFP-Mim1 in *get1Δ* or *get3Δ* cells and analysed the protein localization by fluorescence microscopy. Whereas in WT cells ~20% of the cells had ER staining, only a negligible proportion of the *get* mutant cells displayed the GFP signal in the ER (Fig. 3E,F). We further checked the distribution of GFP-Mim1 in WT and *get* mutants by subcellular fractionation. Importantly, the amount of GFP-Mim1 in the ER was

significantly reduced in the *get* deletion strains (Fig. 3G-I). The presence of a residual ER population of the protein, despite deletion of GET components, suggests that the GET pathway is not the only route for GFP-Mim1 targeting to the ER.

Next, we wondered if the mislocalization depends on the presence of the GFP moiety and on its location. To test this, we fused GFP to the C-terminus of Mim1 and analysed the subcellular distribution of the fusion protein. We observed the vast majority of the protein in the mitochondrial fraction, whereas only a minority was mistargeted to the ER (Fig. S2A). Similarly, overexpressed untagged Mim1 was very partially mislocalized to the ER where it was modified in WT, but not in *get3Δ* cells (Fig. S2B). This modification does not appear to be glycosylation (Fig. S2C), and it is not clear to us why we did not observe it in *get3Δ* cells. Of note, the GET machinery does not seem to contribute to the mistargeting of both Mim1 and Mim1-GFP (Fig. S2A,B). This finding is in agreement with the location of the TMS being positioned in the middle of the protein (as in Mim1) or in its N-terminal region (as in Mim1-GFP), rather than in the C-terminal region (as in GFP-Mim1).

Get3 interacts directly with Mcp3 and Mim1

The results described above, suggest that the GET machinery is involved in mistargeting of mitochondrial proteins. To test whether this effect is a direct one, we expressed a His-tagged version of the soluble component Get3 or of its ATP hydrolysis-deficient mutant (D57N) (Stefer et al., 2011), which fails to release substrate proteins, in *E. coli* cells. The purified proteins were incubated with rabbit reticulocyte lysate expressing HA-Mim1 or HA-Mcp3ΔN, or DHFR-HA as a control. Next, a pull-down with anti-HA beads was performed and bound proteins were analysed. While we could detect only minor binding of native Get3 to HA-tagged proteins, the fraction of bound Get3 was much larger for the ATP hydrolysis-deficient mutant D57N (Fig. 4A,B). Of note, none of the Get3 variants was bound to the control protein, DHFR. Thus, these results indicate that Get3 is able to bind *in vitro* to mitochondrial proteins.

To substantiate these findings by an *in vivo* approach, we employed the cytosolic Split-Ubiquitin System (Asseck et al., 2018; Xing et al., 2016). To this end, we used Get3 as a bait, whereas Mcp3ΔN or GFP-Mcp3ΔN were utilized as preys. Indeed, using these combinations, we observed growth of the yeast cells on stringent Met-containing growth medium, whereas the usage of the negative control NubG as a prey did not result in growth under these conditions (Fig. 4C). Hence, we conclude that Get3 is able to interact *in vivo* with Mcp3.

Conclusions

Our study shows that, when allowed to, the GET pathway is able to recognize newly synthesized mitochondrial proteins. However, this capacity becomes relevant only when the mitochondrial import is compromised. Under normal conditions, the high efficiency and fast kinetics of the mitochondrial import apparatus do not provide factors involved in ER-targeting routes with the option to successfully compete for such interactions. This implies that correct intracellular targeting is dictated by a kinetic competition among various potential pathways.

MATERIALS AND METHODS

Yeast strains and growth conditions

Yeast strains used in the study were isogenic to *Saccharomyces cerevisiae* strain W303α or BY4741. Standard genetic techniques were used for growth and manipulation of yeast strains.

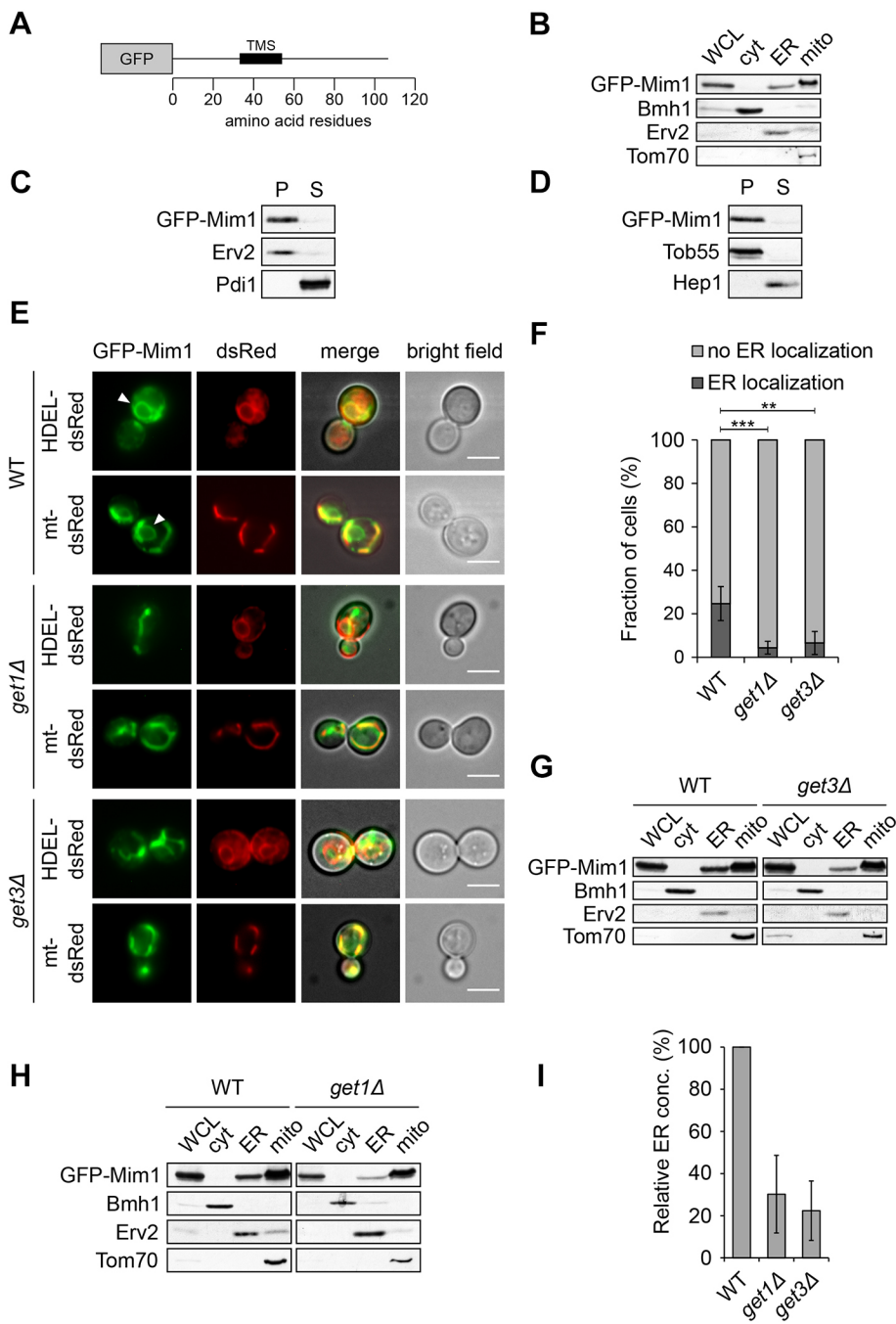


Fig. 3. GET proteins are involved in the mislocalization of GFP-Mim1 to ER. (A) Schematic representation of GFP-Mim1. (B-D) Western blot showing cells expressing GFP-Mim1 subjected to subcellular fractionation (B). (C,D) Western blots of ER (C) and mitochondrial (D) fractions subjected to alkaline extraction. (E) WT, *get1Δ*, and *get3Δ* cells expressing GFP-Mim1 were analysed by fluorescence microscopy as described in the legend to Fig. 2D. Scale bars: 5 μm. (F) Quantification of the intracellular localization of GFP-Mim1 monitored as in E and analysed as described in the legend to Fig. 2E. ***P*≤0.001; ****P*≤0.0001. (G-H) Western blots of WT, *get3Δ* (G), and *get1Δ* (H) cells expressing GFP-Mim1 subjected to subcellular fractionation. (I) Three independent experiments as shown in G and H were quantified, and the enrichment of GFP-Mim1 in ER fractions are depicted. WCL, whole-cell lysate; cyt, cytosol fraction; ER, microsomes fraction; mito, mitochondria fraction; WT, wild type.

Yeast cells were grown in standard rich medium YP (2% [w/v] bacto peptone, 1% [w/v] yeast extract) or synthetic medium S (0.67% [w/v] bacto-yeast nitrogen base without amino acids) with either glucose (2% [w/v], D) or galactose (2% [w/v], Gal) as carbon source. Transformation of yeast cells was performed by the lithium acetate method.

To delete the complete ORFs of *GET1*, *GET2* or *GET3*, they were replaced with KanMX4, CloNAT or Ble cassettes amplified with gene-specific primers. The deletions were confirmed by PCR. The GFP-tag at the N-terminus of the *MCP3* ORF was genomically inserted and encoded under the *SpNOP1* promoter. A GFP-moiety was inserted upstream of the *MIM1* ORF and the fusion protein was expressed under the control of the *ADH* promoter. Table S1 includes a list of strains used in this study.

Recombinant DNA techniques

The cDNAs of rabbit cytochrome b5 ER and its RR variant were amplified by PCR with primers containing EcoRI and HindIII restriction sites from

pGEM4-b5ER and pCDNA3-b5RR, respectively (Borgese et al., 2001). The obtained DNA fragments were inserted in-frame with an N-terminal 3HA-tag that was cloned between EcoRI and NcoI sites, into the multi-copy yeast expression plasmid pYX223 (*GAL* promoter). To obtain pGEM4-yk-DHFR-3HA, the DHFR coding sequence was amplified from pGEM4-pSu9-DHFR with primers containing KpnI and BamHI restriction sites as well as the yeast Kozak sequence, and inserted into the pGEM4 plasmid in-frame with a C-terminal 3HA-tag cloned into BamHI and Sall restriction sites.

Plasmid pRS426-TPI-GFP-Mcp3ΔN was obtained by PCR amplification from genomic DNA, of the sequence coding for the 126 most C-terminal amino acids of Mcp3, with primers containing BamHI and HindIII restriction sites. The obtained DNA fragment was inserted in the pRS426-TPI vector in-frame with an N-terminal GFP cloned between two EcoRI sites. The *MCP3ΔN* coding sequence was subcloned, by using BamHI and HindIII restriction enzymes, from this plasmid into a pGEM4 vector

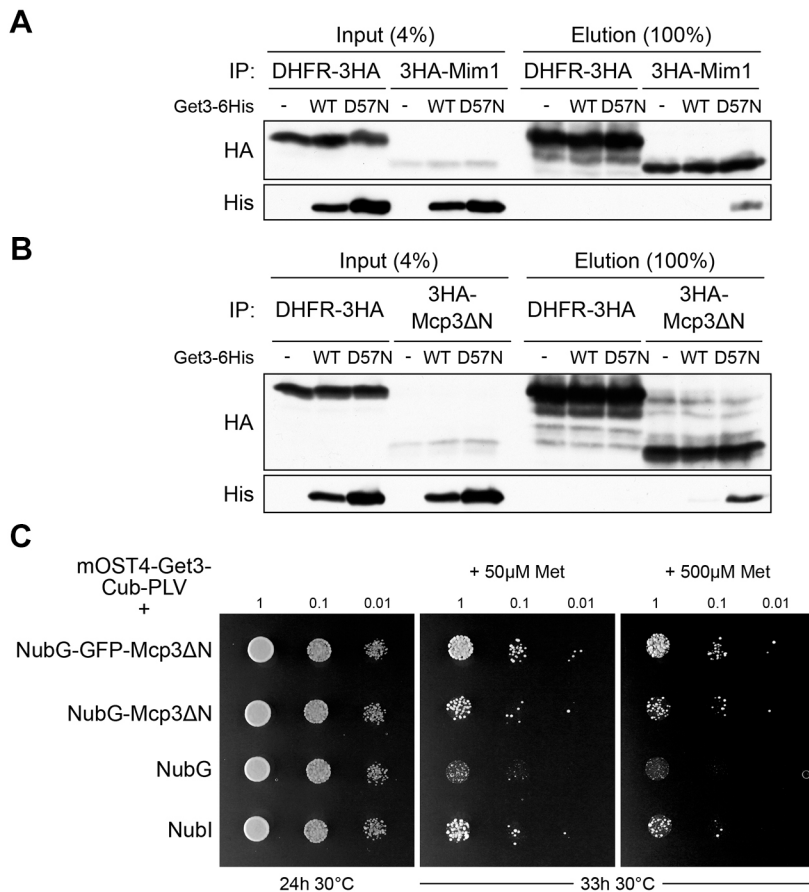


Fig. 4. Get3 physically interacts with Mcp3 and Mim1. (A,B) The indicated radiolabelled HA-tagged proteins were incubated with buffer only (-) or with His-tagged versions of either native Get3 (WT) or the D57N variant. The mixtures were pulled-down with anti-HA beads. Samples from the input and the eluates were analysed by SDS-PAGE and immunoblotting. (C) The cytoSUS was used to monitor interaction of Get3 (used as bait) with Mcp3ΔN (used as prey) with or without GFP-tag together with controls (NubG, negative; Nubl, positive). Diploid yeast cells were dropped at OD₆₀₀ of 1.0, 0.1 and 0.01 on complete supplement mixture (CSM) medium to verify mating and on CSM with either 50 or 500 μM methionine to test for the specificity of interaction.

containing the yeast Kozak sequence and an N-terminal 3HA-tag between EcoRI and KpnI sites. The ORF coding for Mim1 was amplified by PCR from pRS426-TPI-MIMI with primers containing restriction sites BamHI and HindIII, and four Met residues at the C-terminus. The obtained fragment was inserted in-frame with an N-terminal 3HA-tag, which was cloned between the EcoRI and KpnI restriction sites, into a pGEM4 vector containing the yeast Kozak sequence. To obtain the construct Mim1-GFP, the MIMI ORF without a stop codon was PCR amplified with primers containing EcoRI and BamHI restriction sites. Then, the PCR product was treated with both restriction enzymes and was inserted into the pRS426-TPI vector in-frame with a C-terminal GFP, which was inserted between KpnI and HindIII restriction sites. Similarly, the MIMI ORF was inserted into the pYX223 vector using EcoRI and HindIII.

Biochemical methods

Protein samples for immunoblotting were analysed on 12.5% or 15% SDS-PAGE and subsequently transferred onto nitrocellulose membranes by semi-dry western blotting. Proteins were detected by incubating the membranes, first with primary antibodies and then with horseradish peroxidase-conjugates of goat anti-rabbit or goat anti-rat secondary antibodies. Band intensities were quantified using the AIDA software (Elysia-raytest, Straubenhardt, Germany). Enrichment in the ER fraction was calculated by dividing the signal for the protein of interest in the ER fraction by that in the whole-cell lysate. This value was then divided by the same ratio calculated for the marker ER protein, Erv2 or Sec61 (protein X in ER/protein X in WCL)/(Erv2 or Sec61 in ER/Erv2 or Sec61 in WCL).

Subcellular fractionation was performed as described before (Walther et al., 2009). Isolation of mitochondria from yeast cells was performed by differential centrifugation, as previously described (Daum et al., 1982). To obtain highly pure mitochondria, isolated organelles were layered on top of a Percoll gradient and isolated according to a published procedure (Graham, 2001).

For protease protection assay, 50 μg of microsomes were resuspended in 100 μl of SEM buffer (250 mM sucrose, 1 mM EDTA, 10 mM MOPS pH

7.2). As a control, microsomes were treated with 1% Triton X-100 in SEM buffer and incubated on ice for 30 min. The samples were supplemented with proteinase K (50 μg/ml) and incubated on ice for 30 min. The proteolytic reaction was stopped with 5 mM phenylmethylsulfonyl fluoride (PMSF). The samples were precipitated with trichloroacetic acid (TCA) and resuspended in 40 μl of 2× Laemmli buffer, heated for 10 min at 50°C, and analysed by SDS-PAGE and immunoblotting.

To analyse the membrane topology of proteins, alkaline extraction was performed. Mitochondria or ER fractions (50 μg) were resuspended in 100 μl of buffer containing 10 mM HEPES-KOH pH 11.5 with 100 mM Na₂CO₃, and incubated on ice for 30 min. The membrane fraction was pelleted by centrifugation (76,000 g, at 2°C for 30 min) and the supernatant fraction was precipitated with TCA. Both fractions were resuspended in 40 μl of 2× Laemmli buffer, heated for 10 min at 50°C or 95°C, and analysed by SDS-PAGE and immunoblotting.

The following proteins were used as marker proteins in western blots shown in Figs 1-4: Bmh1, a cytosolic protein; Erv2, an ER membrane protein exposed to the ER lumen; Fis1, a mitochondrial membrane protein; Hep1, a soluble mitochondrial protein; Om14, a mitochondrial membrane protein; Pdi1, a soluble glycosylated ER protein; Tom70, a mitochondrial membrane protein; Sec61, an ER membrane protein; Tob55, a mitochondrial membrane protein; Tom40, a MOM protein. Table S1 includes a list of the antibodies used in this study.

In vitro interactions of recombinant Get3

Plasmids encoding His-tagged versions of Get3 and of its ATP hydrolysis-deficient mutant (D57N) were a kind gift from Irmgard Sinning. Proteins were expressed in *E. coli* cells and purified as described previously (Stefer et al., 2011). 3HA-Mim1, 3HA-Mcp3ΔN or DHFR-3HA were translated *in vitro* in rabbit reticulocyte lysate in the presence of 10 mM DTT and 5 μM of recombinant Get3-6His or Get3D57N-6His. After translation, the lysate was diluted with KHM buffer (110 mM KAc, 20 mM HEPES-KOH pH 7.4, 2 mM MgCl₂) supplemented with 50 mM ATP. Then, the lysate was added

to magnetic anti-HA beads (10 μ l) that had been equilibrated with KHM buffer for 30 min at 4°C, and incubated with them for 2 h at 4°C. The beads were washed four times with KHM buffer and bound proteins were eluted at either 95°C or 50°C for 10 min with 100 μ l of 2 \times Laemmli buffer lacking β -mercaptoethanol but supplemented with 5% H₂O₂. Samples were analysed by SDS-PAGE and immunoblotting.

Glycosylation assay

To test for glycosylation of proteins, 50 μ g of the ER fraction was resuspended in 10 μ l glycoprotein denaturing buffer (0.5% SDS, 40 mM DTT) and incubated for 10 min at 95°C. Then, the samples were supplemented with 500 units of either endoglycosidase H (EndoH) or peptide:N-glycosidase F (PNGase) (New England BioLabs) in the respective buffer (according to the manufacturer's instructions) and incubated for 1 h at 37°C. At the end of the incubation period, the samples were precipitated with TCA, resuspended in 40 μ l of 2 \times Laemmli buffer, heated for 10 min at either 50°C or 95°C, and analysed by SDS-PAGE and immunoblotting.

The yeast cytosolic split-ubiquitin system

The yeast cytosolic split-ubiquitin system (cytoSUS) was used to detect physical interaction. The bait protein Get3 was expressed from the Met25 promoter, N-terminally fused to the transmembrane domain of OST4p (mOST4) to ensure membrane anchoring and C-terminally tagged with the C-terminal ubiquitin moiety (Cub) followed by the chimeric ProteinA-LexA-VP16 (PLV) transcription activator (Xing et al., 2016). The bait fusion was transformed in the *S. cerevisiae* strain THY.AP4. N-terminally NubG-2 \times HA-tagged prey proteins GFP-Mcp3 Δ N and Mcp3 Δ N, as well as the control peptides NubG (as a positive control) and NubI (wild-type Nub, as a positive control) were transformed in the *S. cerevisiae* strain THY.AP5. After mating, diploids were selected. Interaction analysis was performed by spotting serial dilutions of diploid yeast on interaction-selective complete supplement mixture (CSM) medium lacking adenine and histidine but containing increasing concentrations of methionine (50–500 μ M) to decrease bait expression. Protein expression was verified by western blotting utilizing anti-VP16 antibody (rabbit, GeneTex) for bait and anti-HA peroxidase-conjugated (Roche) antibody for prey fusions as described previously (Asseck et al., 2018; Xing et al., 2016).

Fluorescence microscopy

Fluorescence images were acquired using a spinning disk microscope (Zeiss Axio Examiner Z1) equipped with a CSU-X1 real-time confocal system (Visitron), VS-Laser system and SPOT Flex CCD camera (Visitron Systems). Images were analysed with VisiView software (Visitron). Microscopy images of strains expressing GFP-Mim1 were acquired with an Axioskop 20 fluorescence microscope equipped with an AxioCam MRm camera using the 43 Cy3 filter set and the AxioVision software (Carl Zeiss).

Acknowledgements

We thank E. Kracker for excellent technical assistance and Irmgard Sinning, Biochemistry Center (BZH), Heidelberg, Germany, for plasmids.

Competing interests

The authors declare no competing or financial interests.

Author contributions

Conceptualization: D.G.V., C.G., B.S., N.B., D.R.; Methodology: D.G.V., E.P.B., M. Sinzel, A.K., S.Z., D.G.M., A.C., A.F., B.F.C., C.G., D.R.; Formal analysis: D.R.; Investigation: D.G.V., E.P.B., M. Sinzel, A.K., S.Z., A.C., B.F.C., C.G.; Resources: A.C., A.F., M. Schuldiner, B.S., N.B., D.R.; Data curation: E.P.B., M. Sinzel, A.K., S.Z., D.G.M., C.G.; Writing - original draft: D.G.V., M. Schuldiner, B.S., N.B., D.R.; Writing - review & editing: C.G.; Supervision: B.S., N.B., D.R.

Funding

This work was supported by the Deutsche Forschungsgemeinschaft (Sonderforschungsbereich 1190-TP04 to B.S.; RA 1028/7-1 to D.R.; Deutsch-Israelische Projektkooperation to D.R. and M. Schuldiner; and GR 4251/2-1 to C.G.), and the ITN TAMpting network to D.G.V., B.F.C., B.S., N.B. and D.R. [funded by the

People Programme (Marie Curie Actions) of the European Union's Seventh Framework Programme FP7/2007-2013/ under REA grant agreement no 607072].

Supplementary information

Supplementary information available online at <http://jcs.biologists.org/lookup/doi/10.1242/jcs.211110.supplemental>

References

- Asseck, L. Y., Wallmeroth, N. and Grefen, C. (2018). ER membrane protein interactions using the Split-Ubiquitin System (SUS). *Methods Mol. Biol.* **1691**, 191-203.
- Aviram, N., Ast, T., Costa, E. A., Arakel, E. C., Chuartzman, S. G., Jan, C. H., Haßdenteufel, S., Dudek, J., Jung, M., Schorr, S. et al. (2016). The SND proteins constitute an alternative targeting route to the endoplasmic reticulum. *Nature* **540**, 134-138.
- Borgese, N. and Fasana, E. (2011). Targeting pathways of C-tail-anchored proteins. *Biochim. Biophys. Acta* **1808**, 937-946.
- Borgese, N., Gazzoni, I., Barberi, M., Colombo, S. and Pedrazzini, E. (2001). Targeting of a tail-anchored protein to endoplasmic reticulum and mitochondrial outer membrane by independent but competing pathways. *Mol. Biol. Cell* **12**, 2482-2496.
- Brambillasca, S., Yabal, M., Soffientini, P., Stefanovic, S., Makarow, M., Hegde, R. S. and Borgese, N. (2005). Transmembrane topogenesis of a tail-anchored protein is modulated by membrane lipid composition. *EMBO J.* **24**, 2533-2542.
- Casson, J., McKenna, M., Haßdenteufel, S., Aviram, N., Zimmerman, R. and High, S. (2017). Multiple pathways facilitate the biogenesis of mammalian tail-anchored proteins. *J. Cell Sci.* **130**, 3851-3861.
- Colombo, S. F., Longhi, R. and Borgese, N. (2009). The role of cytosolic proteins in the insertion of tail-anchored proteins into phospholipid bilayers. *J. Cell Sci.* **122**, 2383-2392.
- D'Arrigo, A., Manera, E., Longhi, R. and Borgese, N. (1993). The specific subcellular localization of two isoforms of cytochrome b5 suggests novel targeting pathways. *J. Biol. Chem.* **268**, 2802-2808.
- Daum, G., Böhni, P. C. and Schatz, G. (1982). Import of proteins into mitochondria: cytochrome b2 and cytochrome c peroxidase are located in the intermembrane space of yeast mitochondria. *J. Biol. Chem.* **257**, 13028-13033.
- Dukanovic, J. and Rapaport, D. (2011). Multiple pathways in the integration of proteins into the mitochondrial outer membrane. *Biochim. Biophys. Acta* **1808**, 971-980.
- Egan, B., Beilharz, T., George, R., Isenmann, S., Gratzer, S., Wattenberg, B. and Lithgow, T. (1999). Targeting of tail-anchored proteins to yeast mitochondria in vivo. *FEBS Lett.* **451**, 243-248.
- Fueller, J., Egorov, M. V., Walther, K. A., Sabet, O., Mallah, J., Grabenbauer, M. and Kinkhabwala, A. (2015). Subcellular partitioning of protein tyrosine phosphatase 1B to the endoplasmic reticulum and mitochondria depends sensitively on the composition of its tail anchor. *PLoS ONE* **10**, e0139429.
- Graham, J. M. (2001). Isolation of mitochondria from tissues and cells by differential centrifugation. *Curr. Prot. Cell Biol.* Chapter 3: 3.3.1-3.3.15.
- Hassdenteufel, S., Sicking, M., Schorr, S., Aviram, N., Fecher-Trost, C., Schuldiner, M., Jung, M., Zimmermann, R. and Lang, S. (2017). hSnd2 protein represents an alternative targeting factor to the endoplasmic reticulum in human cells. *FEBS Lett.* **591**, 3211-3224.
- Ishikawa, D., Yamamoto, H., Tamura, Y., Moritoh, K. and Endo, T. (2004). Two novel proteins in the mitochondrial outer membrane mediate β -barrel protein assembly. *J. Cell Biol.* **166**, 621-627.
- Kalbfleisch, T., Cambon, A. and Wattenberg, B. W. (2007). A bioinformatics approach to identifying tail-anchored proteins in the human genome. *Traffic* **8**, 1687-1694.
- Kemper, C., Habib, S. J., Engl, G., Heckmeyer, P., Dimmer, K. S. and Rapaport, D. (2008). Integration of tail-anchored proteins into the mitochondrial outer membrane does not require any known import components. *J. Cell Sci.* **121**, 1990-1998.
- Krumpe, K., Frumkin, I., Herzig, Y., Rimon, N., Özbalci, C., Brügger, B., Rapaport, D. and Schuldiner, M. (2012). Ergosterol content specifies targeting of tail-anchored proteins to mitochondrial outer membranes. *Mol. Biol. Cell* **23**, 3927-3935.
- Rao, M., Okreglak, V., Chio, U. S., Cho, H., Walter, P. and Shan, S.-O. (2016). Multiple selection filters ensure accurate tail-anchored membrane protein targeting. *eLife* **5**, e21301.
- Schuldiner, M., Metz, J., Schmid, V., Denic, V., Rakwalska, M., Schmitt, H. D., Schwappach, B. and Weissman, J. S. (2008). The GET complex mediates insertion of tail-anchored proteins into the ER membrane. *Cell* **134**, 634-645.
- Sinzel, M., Tan, T., Wendling, P., Kalbacher, H., Özbalci, C., Chelius, X., Westermann, B., Brügger, B., Rapaport, D. and Dimmer, K. S. (2016). Mcp3 is a novel mitochondrial outer membrane protein that follows a unique IMP-dependent biogenesis pathway. *EMBO Rep.* **17**, 965-981.
- Stefer, S., Reitz, S., Wang, F., Wild, K., Pang, Y.-Y., Schwarz, D., Bomke, J., Hein, C., Lohr, F., Bernhard, F. et al. (2011). Structural basis for tail-anchored

- membrane protein biogenesis by the Get3-receptor complex. *Science* **333**, 758-762.
- Waizenegger, T., Schmitt, S., Zivkovic, J., Neupert, W. and Rapaport, D.** (2005). Mim1, a protein required for the assembly of the TOM complex of mitochondria. *EMBO Rep.* **6**, 57-62.
- Walther, D. M., Papic, D., Bos, M. P., Tommassen, J. and Rapaport, D.** (2009). Signals in bacterial β -barrel proteins are functional in eukaryotic cells for targeting to and assembly in mitochondria. *Proc. Natl. Acad. Sci. USA* **106**, 2531-2536.
- Wang, F., Brown, E. C., Mak, G., Zhuang, J. and Denic, V.** (2010). A chaperone cascade sorts proteins for posttranslational membrane insertion into the endoplasmic reticulum. *Mol. Cell* **40**, 159-171.
- Wang, F., Whynot, A., Tung, M. and Denic, V.** (2011). The mechanism of tail-anchored protein insertion into the ER membrane. *Mol. Cell* **43**, 738-750.
- Xing, S., Wallmeroth, N., Berendzen, K. W. and Grefen, C.** (2016). Techniques for the Analysis of Protein-Protein Interactions in Vivo. *Plant Phys.* **171**, 727-758.